Precision Engineering 49 (2017) 344–353

Contents lists available at ScienceDirect

Precision Engineering

journal homepage: www.elsevier.com/locate/precision

An improved accuracy-measuring method in manufacturing the lead screw of grating ruling engine

Xuefeng Yao[a,b,*], Jicheng Cui[a], Haili Yu[a], Xiangdong Qi[a], Xiaotao Mi[a,b], Yimin Jiang[c], Mingjia Wang[a], Xiaotian Li[a]

[a] Changchun Institute of Optics, Fine Mechanics and Physics, Chinese Academy of Sciences, Dongnanhu Road, 3888#, 130033, Changchun, PR China
[b] University of Chinese Academy of Sciences, Yuquan Road, 19#A, 100049, Beijing, PR China
[c] The Civil Aviation of China, Jinbei Road, 2898#, 300300, Tianjin, PR China

ARTICLE INFO

Article history:
Received 22 December 2016
Received in revised form 13 March 2017
Accepted 16 March 2017
Available online 24 March 2017

Keywords:
Lead screw
Grating ruling engine
Axial displacement
Error analysis
Non-contact measurement
Laser interferometer

ABSTRACT

A measuring method was studied to further improve the manufacturing accuracy of the lead screw. Firstly, factors that can axially displace the screw shaft were analyzed and a relationship between factors and axial displacement was given. The axial displacement of the screw shaft was measured using a laser interferometer, and results show that the variation amplitude of the screw-shaft axial displacement was about 80 nm while the variation period was consistent with the rotation period of the screw shaft. Next, two methods of measuring the manufacturing accuracy of the lead screw were considered: a traditional method that measures the absolute position of the nut and an improved method that measures the displacement between the nut and screw shaft. A No. 4 screw shaft was manufactured under the guidance of results obtained using the improved measuring method. Experimental measurements were then made; results show that the pitch displacement errors obtained using the traditional and improved measuring methods were 0.6 and 0.4 μm, respectively, indicating that the improved measuring method is more exact. Finally, an echelle grating ruled by a grating ruling engine that used the No. 4 screw shaft as a macro-positioning element was introduced. Its excellent parameters indirectly show that the improved measuring method has better accuracy.

1. Introduction

With the development of micro-displacement technology, new positioning technologies, represented by piezoelectric ceramics, have been developed in recent years [1]. These technologies can reach the nanometer level of position accuracy, but they also have shortcomings, such as a small travel range and weak bearing capacity [2,3]. The traditional lead screw drive form therefore remains irreplaceable in some large-travel and heavy-load-transmission applications. The positioning accuracy of the lead screw is usually at the micron level. However, for large-travel precision instruments, such as grating ruling engines, diamond lathes and ultra-precision grinding machines, the required positioning accuracy is usually tens of nanometers, and it is difficult to reach this precision level using the lead screw drive alone [4,5]. For these instruments, the usual practice is to position the lead screw as a macro positioning element and to realize an accuracy of tens of nanometers using micro positioning devices, such as those made from piezoelectric ceramics [6,7]. The precision of the macro positioning will directly affect the control accuracy and difficulty of micro positioning, which is more obvious in the case of an open-loop control system [8]. How to improve the positioning accuracy of the lead screw has therefore become an important challenge for engineers and technicians to overcome.

Generally speaking, methods of manufacturing lead screws can be divided into three types: cutting, grinding and lapping methods. Most ultra-precision lead screws are manufactured by lapping at present. In the lapping process, the transmission accuracy of the lead screw must be measured frequently, and the measurement results are used as feedback to guide the lapping of the lead screw [9–14]. A high-precision measuring method is therefore indispensable to obtaining a high-precision lead screw. Large-travel and nanometer-level-accuracy measurement has become possible in recent years with the emergence of laser interferometer technology, which is being increasingly adopted by lead screw measuring machines [15–17]. According to conventional engineering experi-

* Corresponding author at: Changchun Institute of Optics, Fine Mechanics and Physics, Chinese Academy of Sciences, Dongnanhu Road, 3888#, 130033, Changchun, PR China.
E-mail address: yaoxf@ciomp.ac.cn (X. Yao).

http://dx.doi.org/10.1016/j.precisioneng.2017.03.004
0141-6359/

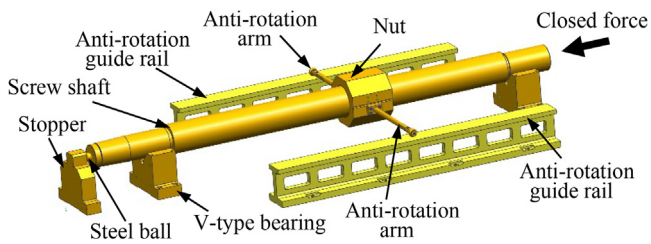

Fig. 1. V-type bearing installation that is widely used for lead screw measuring machines and grating ruling engines.

ence, it is generally believed that the transmission error of a lead screw is mainly due to the pitch distance error and mismatch of the pitch size between the screw shaft and nut. In the past, attempts to improve the transmission accuracy of a lead screw were made by continuously increasing the machining accuracy of the screw shaft and nut, but it was later found that when the machining accuracy reaches a certain level, continuing to improve the precision of manufacturing does not increase the transmission accuracy proportionally, especially in the sub-micron accuracy range. To explain this phenomenon, the present article proposes factors that affect the transmission accuracy of the lead screw from other perspectives and carries out related research.

The remainder of the paper is organized as follows. Section 2 introduces the V-type bearing installation of the screw shaft and the error analysis of deviation and nonperpendicularity is carried out. Section 3, on the basis of the laser interferometer, presents an optical schematic of a device used to measure the axial displacement of a screw shaft. Section 4 discusses the effect of the measurement environment and sets up the screw shaft axial-displacement system. After a method of adjusting the measurement mirror is introduced, error analysis is performed to calculate the off-axis error, which is the deviation between the center of the optical path and the rotation axis of the screw shaft, and the nonperpendicularity error between the measurement mirror and the rotation axis of the screw shaft. Section 5 measures axial displacements for forward and reverse directions and compares them with the axial runout of assembled radial rolling bearings of difference tolerance classes. Section 6 employs two different methods to measure the transmission accuracy of the lead screw, introduces two optical schematics and the structure of the measuring machine and compares the two measurement results. The measurements reveal a stick-slip motion phenomenon. Conclusions are presented in Section 7.

2. Analysis of the axial displacement of a screw shaft

Fig. 1 is a schematic diagram of the method of installing a lead screw that is widely used for lead screw measuring machines and grating ruling engines. As shown in the figure, the screw shaft is supported by two V-type bearings at the two journals of its, and the nut is connected with two anti-rotation arms that are always in contact with the anti-rotation guide rail to avoid rotating with the screw shaft. To limit the degree of freedom in the axial direction of the screw shaft, a closed force acting leftward is provided together with a steel ball and stopper that are located at the left end of the screw shaft. Under the effect of the closed force, the contact between the steel ball and the stopper is at a point, and the axial clearance that exists in the assembled radial rolling bearings does not exist for the V-type bearing.

Although the V-type bearing installation mentioned above reduces the axial clearance, it does not eliminate axial displacement. Fig. 2 shows how axial displacement occurs. During the process of manufacturing, assembling and adjusting, it is sometimes impossible to avoid deviation between the center of the steel ball and the rotation axis of the screw shaft as well as nonperpendicularity between the limit surface of the stopper and the rotation axis of the screw shaft. We define two coordinate systems for the convenience of analysis. In Fig. 2(a) and (b), the Z-axis is the rotation axis of the screw shaft and the Y-axis is the reverse direction of gravity. For analysis on the limit surface of the stopper, the Y′-axis is directed vertically upward and the X'-axis horizontally rightward, as shown in Fig. 2(c). According to the geometric relationship, if we ignore the size of the steel ball, it is reasonable to believe that the axial displacement of the steel ball is the same as that of the screw shaft. When the screw shaft rotates through one cycle, the ball will travel along an elliptical trajectory on the limit surface of the stopper. As shown in Fig. 2(c), the curve equation of the ellipse can be expressed as

$$\left(\frac{x'}{\delta}\right)^2 + \left(\frac{y' \cdot \cos\theta}{\delta}\right)^2 = 1 \tag{1}$$

where δ is the deviation between the center of the steel ball and the rotation axis of the screw shaft in the direction of the Y′-axis and θ is the angle between the limit surface of the stopper and the normal plane of the rotation axis of the screw shaft. The equation shows that the length of the major axis of the ellipse is 2δ/cosθ and the length of the minor axis of the ellipse is 2δ.

As shown in Fig. 2(a), when the steel ball rotates around the rotation axis of the screw shaft with angular velocity ω, we can deduce the polar-coordinate equation of the spatial trajectory of the steel ball as

$$\begin{cases} x = \delta\cos\omega t \\ y = \delta\sin\omega t \\ z = -\delta\sin\omega t\tan\theta \end{cases} \tag{2}$$

Eq. (2) reveals that the axial displacement of the steel ball varies with the same frequency of the screw shaft rotation, and its amplitude depends on δ and θ but is independent of ω. The trajectories of the steel ball in space and the Z direction are presented in Fig. 3(a) and (b) respectively. Fig. 3 shows that the trajectory of the steel ball in space is an ellipse, in the Z direction, the trajectory of the steel ball is a sinusoidal curve and the period of the steel ball trajectory is consistent with the rotation period of the screw shaft.

3. Optical schematic design for measuring axial displacement

Figs. 4 and 5 are respectively an optical schematic and three-dimensional diagram of the system for measuring the axial displacement of the screw shaft. The measurement mirror is perpendicular to the rotation axis of the screw shaft, the measurement mirror moves with the screw shaft in the axial direction while the reference mirror is fixed and stationary, and S_m is the axial displacement of the screw shaft.

4. Preparation for the measurement of axial displacement

Several factors outside the laser measurement system can affect system accuracy. These factors (i.e., the measurement environment, machine and material temperature and optics installation) and their interrelationships must be understood to predict the performance of the system. Because the system measures only the relative motion between the interferometer and reflector, measurements are not affected by vibration along the beam axis of the laser source or the receiver. When vibration of the laser head displaces the beam (perpendicular to the beam axis) at an interferometer or receiver, the beam signal power can fluctuate. An insufficient beam signal will arrive at the receiver if this fluctuation

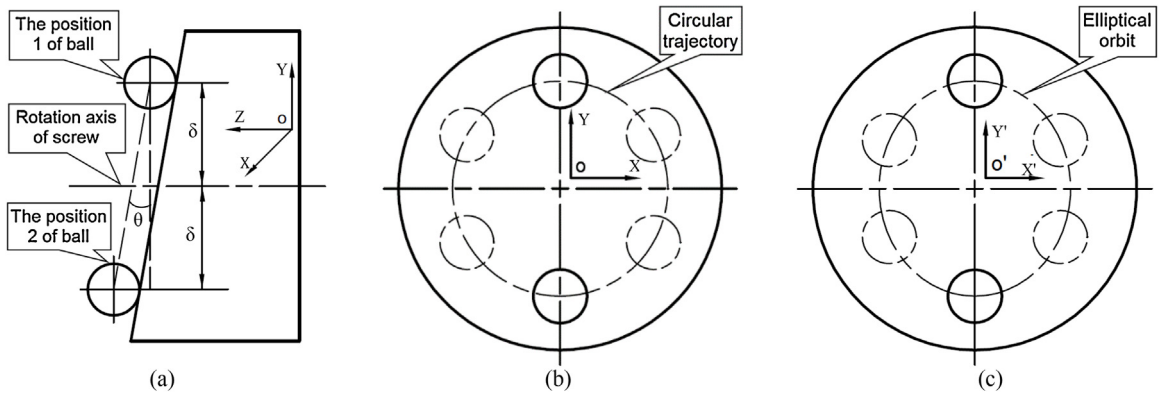

Fig. 2. Axial displacement of the screw shaft: (a) front view, (b) Z-direction view from the left end of the stopper, where the trajectory of the steel ball is a circle, and (c) normal-direction view of the limit surface, where the trajectory of the steel ball is an ellipse.

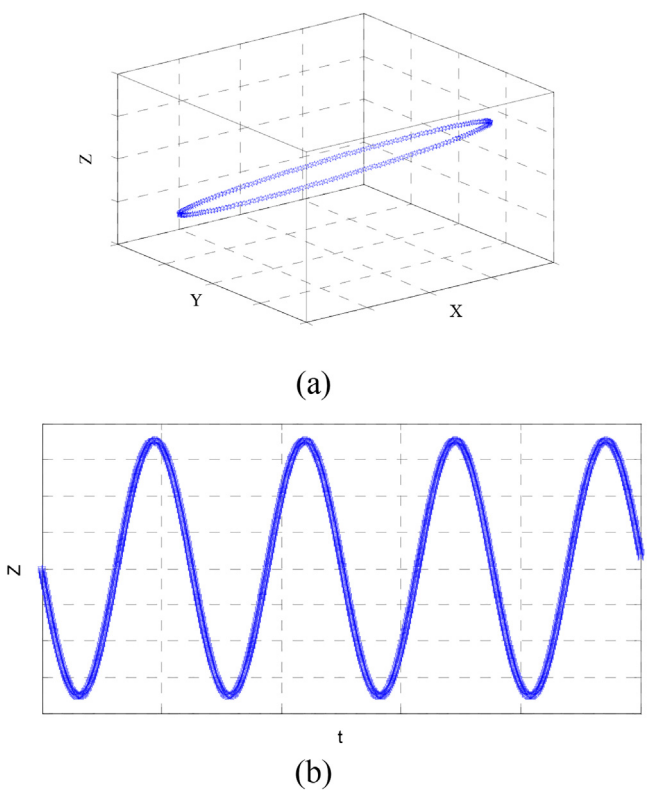

Fig. 3. Results of the theoretical analysis of the steel-ball trajectory, (a) Path traveled by the steel ball as the screw shaft rotates through several cycles, (b) Z component of the path traveled by the steel ball as the screw shaft rotates through several cycles.

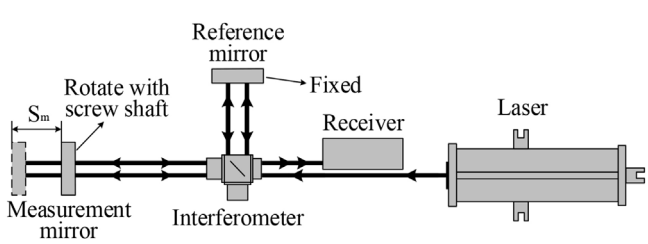

Fig. 4. Optical schematic of the axial displacement measurement system.

is too great, causing a measurement signal error. The above analysis reveals that the environment is crucial to the measurements, and we therefore tested the axial displacement on an air-flotation vibration-isolation platform that isolates high-frequency vibration

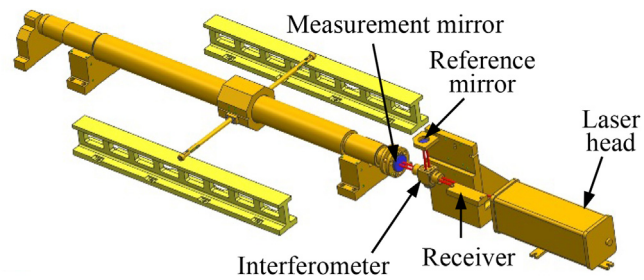

Fig. 5. Three-dimensional diagram of the system used to measure the axial displacement of the screw shaft. For the sake of simplicity, the axial closed force mechanism and the screw shaft driving device are not represented in the figure.

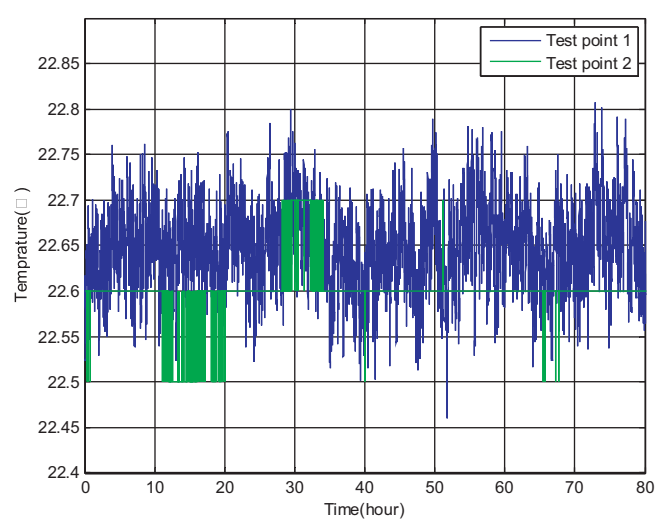

Fig. 6. Temperature monitoring curves of the laboratory recorded continuously for a period of 80 h, which includes the measuring time.

above 5 Hz. The laboratory temperature varied within 22.5 ± 0.5 °C. To monitor the temperature variation, two temperature transducers were placed at two test points in the laboratory. Fig. 6 shows the temperature monitoring result continuously for a period of 80 h, which includes the test time. The blue line is the temperature monitoring curve for monitoring point 1 and the red line is that for monitoring point 2. The figure shows that the temperature variations at the two monitoring points are not more than ±0.5 °C and the average value of the highest temperature and lowest temperature is about 22.65 °C. These parameters meet the environmental requirements of the measuring process.

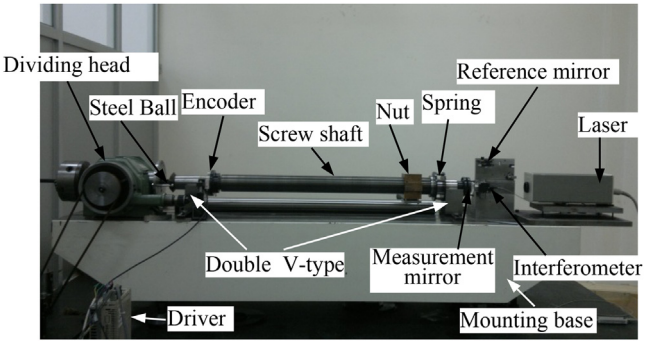

Fig. 7. Photograph of the screw-shaft axial-displacement measurement system; the motor and industrial computer are not included.

The system for measuring the axial displacement of the screw shaft supported by the method described in Section 2 is established. As shown in Fig. 7, the whole measurement system comprises a screw shaft drive module, support module, rotation-angle recording system, axial-displacement recording system and data processing system. The presented measurement method was implemented on a Core 2 Duo 2.80-GHz industrial computer with 2 GB memory. A flow chart of data acquisition and processing is shown in Fig. 8. The data acquisition boards function as the interface over the reading head of the encoder, the receiver of the interferometer and a personal computer. The boards convert the analog electrical voltages from the reading head and receiver to digital forms that the computer uses to calculate the angle and displacement.

An error analysis was conducted before the measurement to analyze the sources of errors and to obtain their degrees of influence. Measurement errors can be divided in three types: measurement system errors, measuring method errors and random errors [18,19]. As the accuracy of the measuring elements are very high, this article mainly focuses on the error caused by non-flatness of the measurement mirror and the alignment error of the measurement system. Fig. 9 is a schematic diagram of measurement error due to off-axis magnitude and nonperpendicularity. As shown in Fig. 9, the spacing of the two beams is 12.7 mm, they are non-centrosymmetrically distributed relative to the rotation axis of the screw shaft. The length of the measuring optical path will vary with the rotation of the screw shaft. During the screw shaft rotates one cycle, the variation is a maximum when the positions of the measurement mirror passes through 180° from position 1 to position 2. The variation of the optical path length M can be expressed as

$$M = \frac{l_1 - l_2}{2} = 2d\tan\alpha \tag{3}$$

where l_1 is the distance from point C to point D, l_2 is the distance from point A to point B, d is the deviation magnitude between the center line of the two beams and the rotation axis of the screw shaft and α is the angle of intersection between the measurement mirror and the normal plane of the rotation axis of the screw shaft.

The non-flatness of the measurement mirror will also affect the measurement accuracy. As shown in Fig. 10(a), the dashed line and the solid line represent the ideal surface and the actual surface of the measurement mirror respectively, and the actual surface has a fluctuation. The term that represents the difference between the highest and lowest points of the measurement mirror is called PV (peak to valley) [20]. According to Eq. (3) and the measurement principle of the interferometer, the related measurement error is half of the PV. In this article, the measurement mirror has been processed by ultra-precision optical polishing, the measurement results of surface shape are shown in Fig. 10(b), and the PV is less

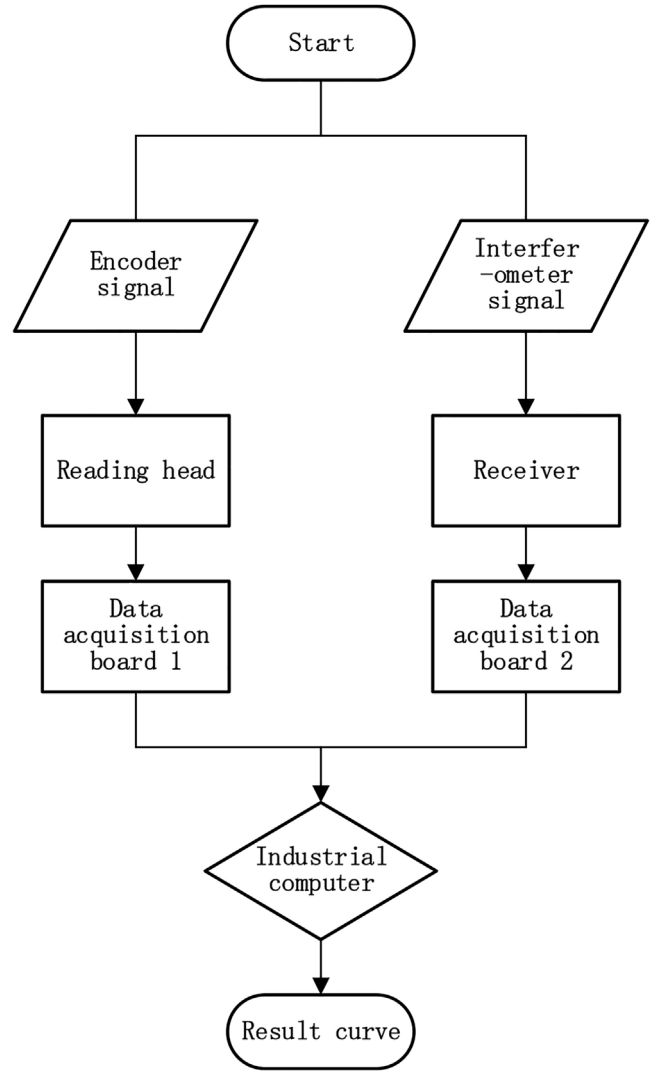

Fig. 8. Flow chart of data acquisition and processing.

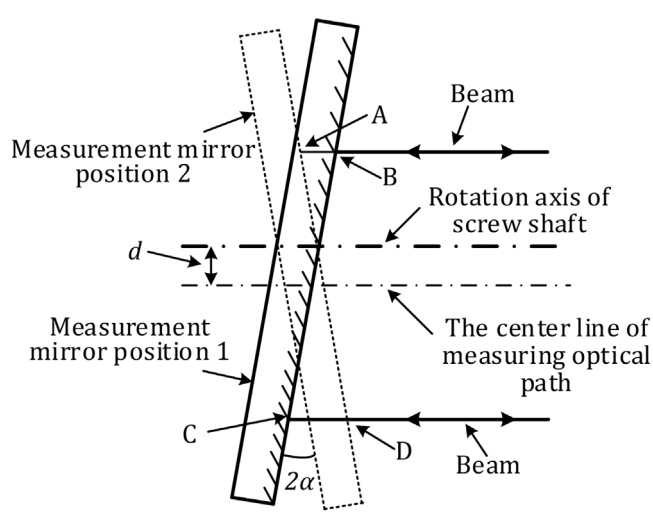

Fig. 9. Schematic diagram of measurement error due to off-axis magnitude and nonperpendicularity.

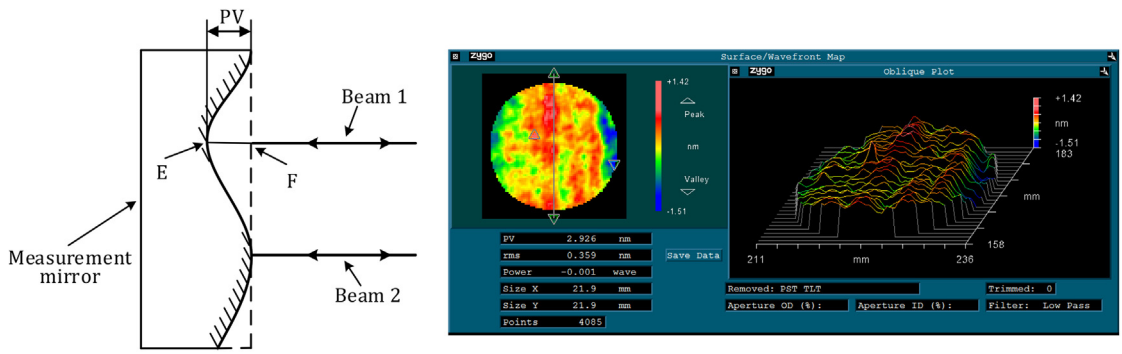

(a) the non-flatness of the measurement mirror (b) the measurement results of surface shape

Fig. 10. The influence of non-flatness on the measurement.

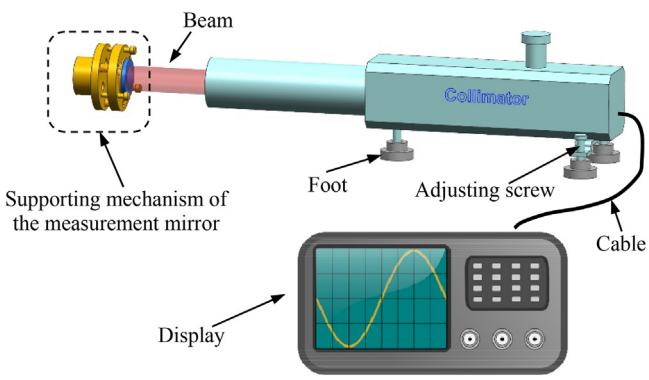

Fig. 11. Schematic diagram of auto-collimation method.

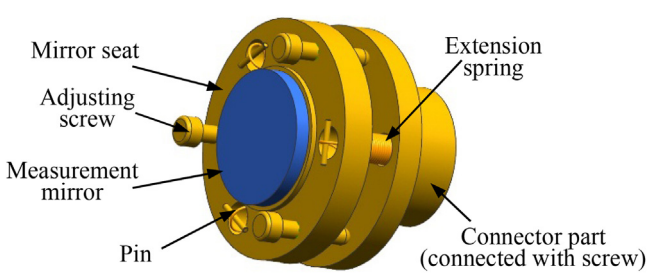

Fig. 12. Partial enlarged drawing of the supporting mechanism of the measurement mirror.

than 3 nm. Thus, the measurement error caused by the non-flatness of the measurement mirror will be less than 1.5 nm.

Before the formal measurement, the surface of the measurement mirror should be adjusted to be perpendicular to the rotation axis of the screw shaft. As shown in Fig. 11, auto-collimation method is employed to adjust the measurement mirror position by three adjusting screws. Fig. 12 is a partial enlarged drawing of the measurement-mirror supporting mechanism, showing that the measurement mirror is fixed by the interaction of three adjusting screws and three extension springs. If the surface of measurement mirror is perpendicular to the rotation axis of the screw shaft, when the screw shaft rotates one cycle, the reading of the autocollimator will remain unchanged. If there is an intersection angle β between the normal plane of the rotation axis of the screw shaft and the surface of measurement mirror, when the screw shaft rotates one cycle, the autocollimator reading will change by β. Thus, when the screw shaft rotates one cycle, the variance of the autocollimator readings is the nonperpendicularity between the surface of measurement mirror and the rotation axis of the screw shaft. When the adjusting screw is adjusted, the pose of the measurement mirror would be changed. Therefore, to make the variance of the autocollimator readings to be less than a certain value, the three screws were adjusted during the rotation of the screw shaft. In this way, the nonperpendicularity between the measurement mirror and the rotation axis of the screw shaft can be adjusted within ±2″.

In order to align the centerline of two measuring beams with the rotation axis of the screw shaft, we designed a jig as shown in Fig. 13(a). At the one side of jig, there is an inner hole which have a tight fit with the journal of the screw shaft. At the other end, two small apertures with the same diameter of the laser beams are arranged on the end face of the jig, the distance between this two apertures is same as the distance between the measuring beam of the interferometer, and they are strictly symmetrical about the axis of the inner hole at the other end. As shown in Fig. 13(b), if the two beams are aligned with two apertures, it is equivalent to align the centerline of the measuring beams with the rotation axis of the screw shaft. Using the alignment jig and method, alignment error will be less than 0.2 mm.

According to the align method mentioned above, the maximum deviation magnitude $d_{\max}$ is 0.2 mm and the maximum intersection angle $\alpha_{\max}$ is 2″. Substituting the above parameters into the expressions for M, the maximum variation of the optical path length caused by "deviation" and "intersection angle" can be obtained as

$$M_{\max} = 2d_{\max}\tan\alpha_{\max} = 3.88\text{nm} \tag{4}$$

The above analysis reveals that the alignment error caused by "deviation" and "intersection angle" is only 3.88 nm and the measurement error caused by non-flatness of the measurement mirror is within 1.5 nm, these errors only have a slight effect on the measurements.

5. Measurements of the axial displacement of the screw shaft

In order to verify the correctness of the analysis conducted in Section 2, the axial displacement of the screw shaft was measured according to the measuring method and measuring system described in Sections 3 and 4. Measurements were carried out in two directions to obtain data that are more scientific. The measurement results are shown in Figs. 14 and 15. The repeatability was visually observed to the two directions measurement results, and the change frequency of the axial displacement is the same as that of the screw shaft rotation, which is consistent with the results of the simulation analysis. Axial displacements of the screw shaft in the two directions were both about 80 nm, this phenomenon is mostly due to the deformation caused by the instability and the poor stiffness of the axial support structure. In practical use, if the

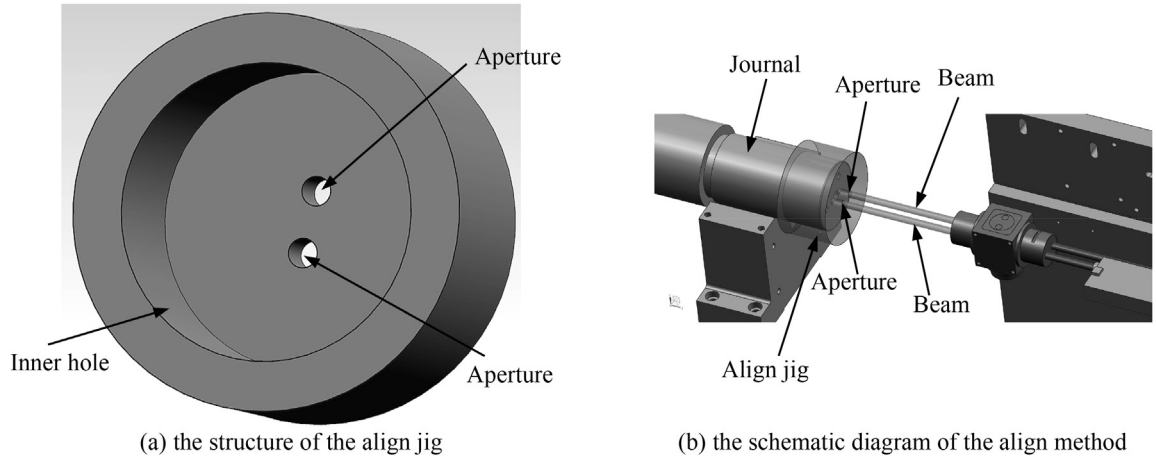

(a) the structure of the align jig (b) the schematic diagram of the align method

Fig. 13. The structure of align jig and the schematic diagram of the align method.

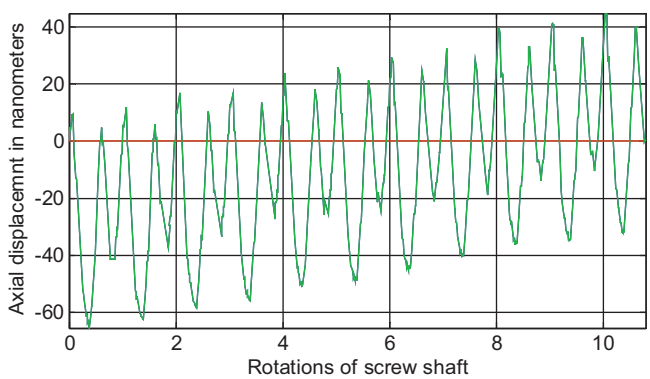

Fig. 14. Results of the screw-shaft axial-displacement test for the forward direction.

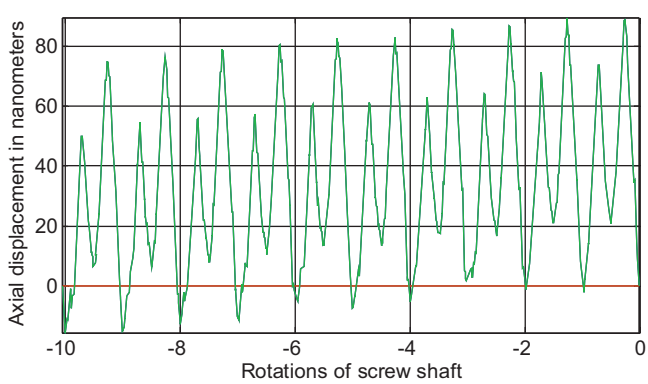

Fig. 15. Results of the screw-shaft axial-displacement test for the reverse direction.

Table 1
The maximum axial runout of the assembled radial rolling bearings with different tolerance class (Tolerance values in micrometers).

Tolerance class	Outer ring	Inner ring
Tolerance class 5	8	7
Tolerance class 4	5	3
Tolerance class 2	1.5	1.5

axial displacement is ignored, a continued increase in machining precision cannot improve the transmission accuracy of the lead screw.

Although the axial displacement is about 80 nm, it is still smaller than that of the rolling bearing. Table 1 gives the maximum axial runout of assembled radial rolling bearings of different tolerance classes that were taken from ISO 492:2014 published by the International Organization for Standardization. The table shows that the maximum axial runout of the assembled radial rolling bearings with the highest tolerance class is 1.5 micrometers, which is about 18 times the axial displacement of the screw shaft supported through the V-type bearings. Therefore, compared with the radial rolling bearing installation method, the V-type bearing installation method is more widely used for precision machines due to its small axial runout.

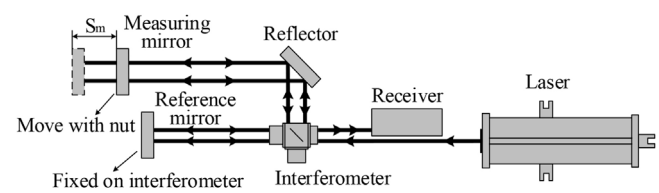

Fig. 16. Optical schematic of the system used to measure the absolute displacement of the nut.

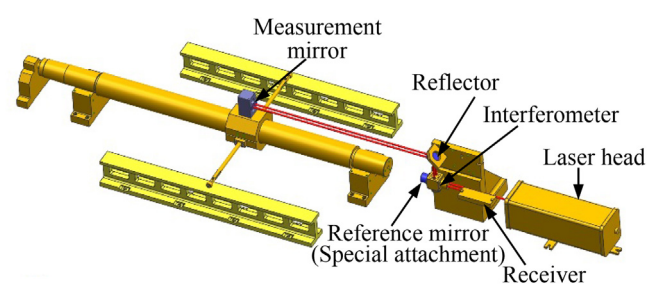

Fig. 17. Three-dimensional diagram of the system used to measure the absolute displacement of the nut, where a special attachment is fixed on the laser interferometer as a reference mirror.

6. Two methods of measuring the manufacturing accuracy of the lead screw

6.1. Traditional measuring method

At present, most accuracy curves are obtained using a traditional method of measuring the absolute position of the nut. Figs. 16 and 17 are the optical schematic and three-dimensional diagram of the traditional measuring machine respectively. In Fig. 16, S_m is the absolute displacement of the nut. From Fig. 17 we can see that during the measurement, if the screw shaft has an axial dis-

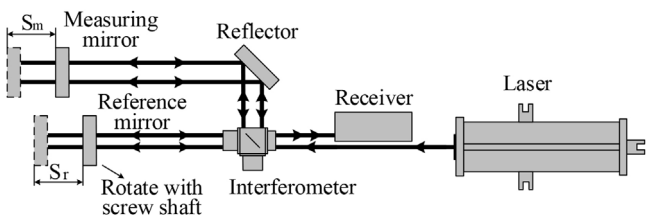

Fig. 18. Optical schematic of the improved system for measuring the accuracy of the lead screw.

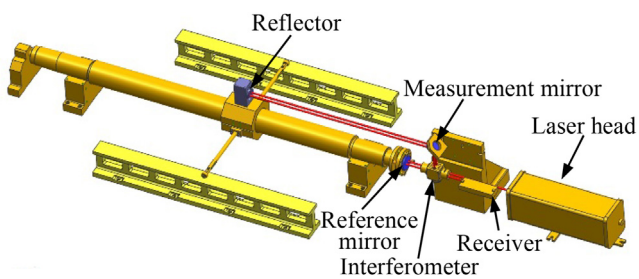

Fig. 19. Three-dimensional diagram of the system for measuring the relative displacement of the nut.

placement, this displacement will be directly transmitted to the nut through the meshing relationship between the screw shaft and nut. We therefore believe that the accuracy curve obtained by measuring the absolute position of the nut does not reflect the transmission accuracy of the lead screw exactly. Poor measurement results obtained by measuring the absolute position of the nut may be due to excessive axial displacement of the screw shaft rather than poor transmission accuracy of the lead screw itself.

6.2. Improved measuring method

We propose an improved measuring method to solve the problem mentioned above. The optical schematic and the three-dimensional diagram of this improved measuring method are shown in Figs. 18 and 19 respectively. The reference mirror perpendicular to the rotation axis of the screw shaft is placed at the end of the screw shaft and rotates with it. When there is displacement in the axial direction, the measurement system obtains the difference between the absolute displacement of the nut and the absolute axial displacement of the screw shaft, which is the relative displacement between the nut and screw shaft, and this physical quantity reflects the transmission precision of the lead screw more exactly. S_d is the relative displacement between the nut and screw shaft in the axial direction and is expressed as

$$S_d = S_m - S_r \tag{5}$$

where S_m is the absolute displacement of the nut and S_r is the absolute axial displacement of the screw shaft.

6.3. Comparison of the two measuring methods

Fig. 20 is a photograph of the measuring machine that is used to obtain the accuracy curves of lead screws. This measuring machine can quickly switch between measuring the absolute position of the nut and measuring the relative position of the nut. The commonality of the two measurement methods is that the measurement mirror is placed on the nut and moves with it. The relative measurements of the nut position are obtained if we place the reference mirror on the end of the screw shaft and perpendicular to the axis of the screw shaft rotation. We can obtain the absolute measurements of the nut position if the special attachment is fixed on the interferometer as a reference mirror.

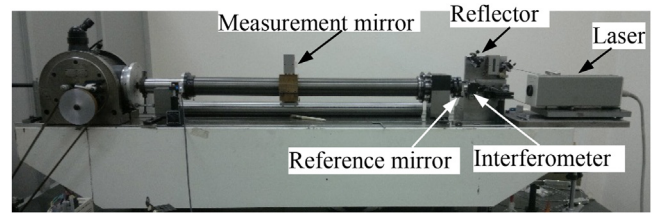

Fig. 20. Photograph of the machine used to measure the lead screw accuracy.

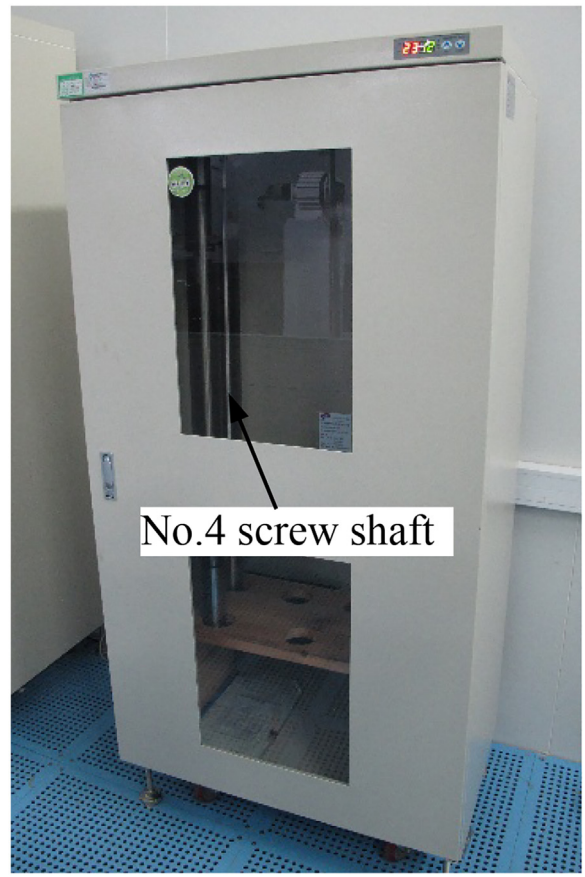

Fig. 21. Photograph of the screw-shaft storage chamber, with the No. 4 screw shaft measured in this study hanging inside.

Fig. 21 is a photograph of a temperature and humidity chamber. A No. 4 screw shaft with a buttress thread hangs in the chamber. The screw shaft was manufactured by lapping under the guidance of the results obtained by measuring the relative displacement between the nut and screw shaft. The final measurement result was obtained after several rounds of lapping alternating with measurement. By contrast, a measurement result was also obtained by measuring the absolute position of the nut as follows.

Figs. 22 and 23 present the accuracy curves obtained by measuring the absolute position of the nut and the relative displacement between the nut and screw shaft respectively. The horizontal axis in each figure gives the rotations of the screw shaft while the vertical axis gives the error value. The figures reveal that the pitch error of the two curves are 0.6 and 0.4 μm respectively, both values are less than 1 μm, indicating that the No. 4 screw shaft has higher accuracy than that of ball screws. Owing to the special design of the measurement optical path, the accuracy curve obtained by measuring the relative displacement between the nut and screw

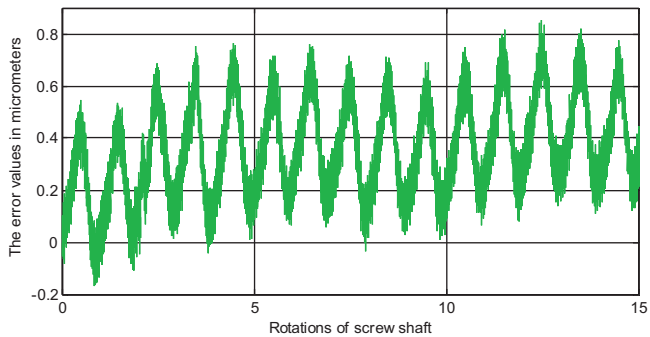

Fig. 22. A period of the accuracy curve obtained by measuring the absolute position of the nut, which contains the axial displacement of the screw shaft, using the traditional measuring method.

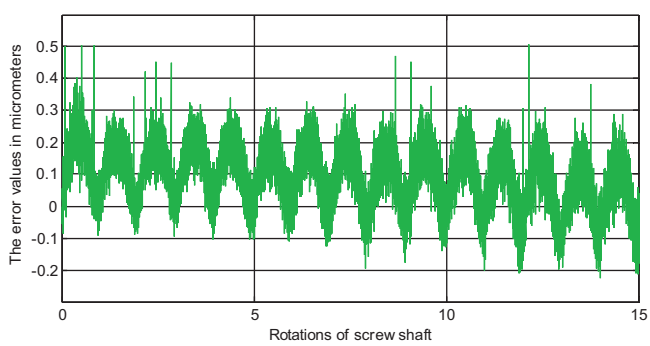

Fig. 23. A period of the accuracy curve obtained by measuring the relative displacement between the nut and screw shaft using the improved measuring method, which can eliminate the axial displacement of the screw shaft.

shaft does not contain the axial displacement of the screw shaft, and it is more exact than the result obtained by measuring the absolute position of the nut. We can infer that the accuracy of the lead screw will become increasingly worse if the lapping continues under the guidance of the measurement result obtained by measuring the absolute position of the nut. Therefore, under the guidance of the measurement result obtained by the improved measurement method, the transmission accuracy of the lead screw manufactured by lapping would be better than that under the guidance of the measurement result obtained by traditional measurement result.

6.4. The practical use of the lead screw manufactured by lapping under the guidance of improved measuring method

After the final lapping, the No. 4 screw shaft was mounted in a Changchun Institute of Optics, Fine Mechanics, and Physics (CIOMP) grating ruling engine, which has the capacity to rule an area of approximately 500 mm × 400 mm, with the 500-mm edge being in the direction of the screw shaft axis. Fig. 24 shows the dividing system of the grating ruling engine, which the No. 4 screw shaft provides macro positioning in the direction of the 500-mm edge.

The grating ruling engine mentioned above successfully ruled a high-quality 79-line/mm echelle grating with an area of 100 mm × 100 mm, Fig. 25 is a photograph of this grating and Fig. 26 shows the diffraction light ($\lambda = 632.8$ nm) of this grating, Fig. 26 shows that there were no obvious Rowland ghosts. The main performance parameters of this 79-line/mm echelle grating are given in Table 2. All of the above indicates that the lead screw which participates the macro-positioning in the CIOMP grating ruling engine has a high accuracy.

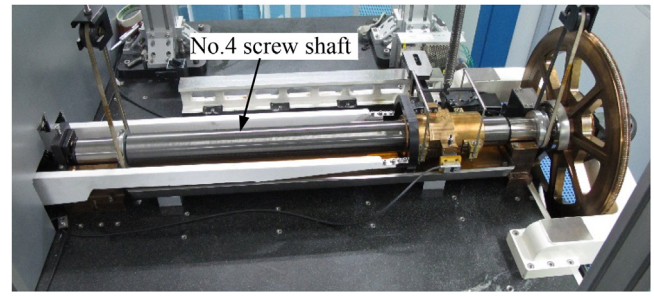

Fig. 24. Dividing system of a grating ruling engine in which a No. 4 screw shaft is installed and provides macro positioning.

Fig. 25. Photograph of an echelle grating with an area of 100 mm × 100 mm.

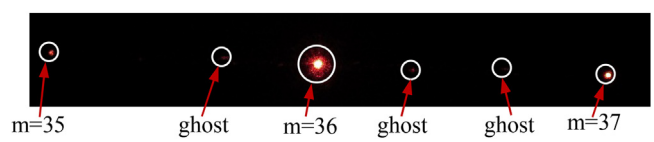

Fig. 26. Diffraction light of a 79-line/mm echelle grating ruled by a grating ruling engine in which a No. 4 screw shaft is mounted.

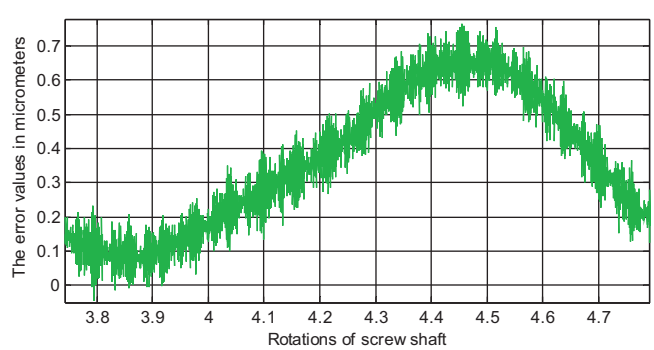

Fig. 27. Partial enlarged drawing of the accuracy curve obtained by measuring the absolute position of the nut.

6.5. The stick-slip motion phenomenon of the lead screw

Figs. 27 and 28 are the partial enlarged drawings of accuracy curves obtained by measuring the absolute position of the nut and the relative displacement between the nut and screw shaft. From Figs. 27 and 28 we can see that the curves consist of many displacement pulses of short duration. This phenomenon is caused by the

Table 2
The main performance parameters of the echelle grating ruled by grating ruling engine which No.4 screw shaft is mounted.

Groove density	Stray light	Diffraction efficiency	Diffraction wavefront
79-line/mm	$<5 \times 10^{-4}$	>50%	$<\lambda/3$

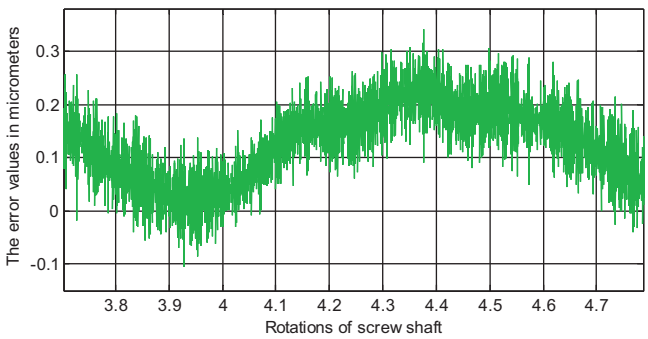

Fig. 28. Partial enlarged drawing of the accuracy curve obtained by measuring the relative displacement between the nut and screw shaft.

frequent alternation of dynamic and static friction between the nut and screw shaft as the screw shaft rotates, this is called the stick-slip motion phenomenon and it has a bad effect on the control of a high-accuracy position system [21–23]. To eliminate the stick-slip motion phenomenon, we should consider how to reduce the friction between the nut and screw shaft as the next step in future research.

7. Conclusion

On the basis of the high-precision, non-contact and real-time measuring ability of the laser interferometer, the present study measured the axial displacement of a screw shaft employing V-type support bearings, which are widely used in measuring machines and grating ruling engines. Measurements show that the axial displacement of the screw shaft has a periodic change, with the period being consistent with the rotation of the screw shaft. The amplitude of the axial displacement is about 80 nm, which would affect the control accuracy of a micro positioning system. Owing to the good periodicity and repeatability of the axial displacement, it is considered possible to add a compensation to the control algorithm and thus improve the control accuracy.

Two measuring methods of the accuracy of the lead screw were discussed in this article and related measurements were carried out on a No. 4 screw shaft. Results show that the pitch error of the lead screw was 0.6 and 0.4 μm for the two measuring methods. Owing to the elimination of the axial displacement of the screw shaft, the result obtained by measuring the relative displacement of the screw shaft and nut is more exact and can provide useful guidance for the manufacturing and alignment of a lead screw.

A No. 4 screw shaft manufactured by lapping under the guidance of results obtained by measuring the relative displacement between the screw shaft and nut was successfully used in a CIOMP grating ruling engine and an echelle grating with an area of 100 mm × 100 mm was fabricated. The main parameters of this echelle grating were excellent. This indirectly verified the correctness and validity of the relative displacement measuring method proposed in this paper.

Further research is needed to improve measurement accuracy and credibility. For example, the Abbe error, screw shaft bending and other factors should be considered in the process of measurement. Although vibration and temperature factors are considered in the measurement, the effect of humidity and pressure variation on the measurement results is neglected. As our next step, we should consider adding wavelength compensation to the measurement process to obtain measurement results that are more accurate and convincing.

Relevant future work, such as reducing the friction between the nut and screw shaft, should be carried out to reduce the effect of the stick-slip motion phenomenon of the lead screw.

Acknowledgments

This work is supported by the National key foundation for exploring scientific instrument of China (Grant No. 2014YQ120351); National Natural Science Foundation of China (Grant No. 61605204, Grant No. 61505204); Jilin Outstanding Youth Project in China (Grant No. 20170520167JH). The authors are also grateful for the help of the colleagues in National Engineering Research Center for Diffraction Gratings Manufacturing and Application.

References

[1] Liu YT, Li BJ. A 3-axis precision positioning device using PZT actuators with low interference motions. Precis Eng 2016;46:118–28.
[2] Cai K, Tian Y, Wang F, Zhang D, Liu X, Shirinzadeh B. Design and control of a 6-degree-of-freedom precision positioning system. Rob Comput Integr Manuf 2017;44:77–96.
[3] Wang C, Xu LL, Zhu J, Yuan ZW, Yu YJ, Asundi AK. A novel integrated fiber-optic interferometer model and its application in micro-displacement measurement. Opt Laser Eng 2016;86:125–31.
[4] Lei B, Wang W, Wu YT, Ma CF, Wang JF, Zhang L, et al. Development and experimental study on a single screw expander integrated into an organic rankine cycle. Energy 2016;116:43–52.
[5] Zhang J, Zhang H, Du C, Zhao W. Research on the dynamics of ball screw feed system with high acceleration. Int J Mach Tools Manuf 2016;111:9–16.
[6] Kim HS, Jeong KS, Dai GL. Design and manufacture of a three-axis ultra-precision CNC grinding machine. J Mater Process Technol 1997;71(2):258–66.
[7] Kita T, Harada T. Ruling engine using a piezoelectric device for large and high-groove density gratings. Appl Opt 1992;31(10):1399–406.
[8] Mo JS, Qiu ZC, Wei JY, Zhang XM. Adaptive positioning control of an ultrasonic linear motor system. Rob Comput Integr Manuf 2017;44:156–73.
[9] Harrison GR, Thompson SW. Large diffraction gratings ruled on a commercial measuring machine controlled interferometrically. J Opt Soc Am 1970;60(5):591–5.
[10] Harrison GR. The production of diffraction gratings I. Development of the ruling art. J Opt Soc Am 1949;39(6):413–26.
[11] Harrison GR, Stroke GW. Interferometric control of grating ruling with continuous carriage advance. J Opt Soc Am 1955;45(2):112–20.
[12] Harrison GR, Thompson SW, Kazukonis H, Connell JR. 750-mm ruling engine producing large gratings and echelles. J Opt Soc Am 1972;62(6):751–6.
[13] Harrison GR, Sturgis N, Davis SP, Yamada Y. Interferometrically controlled ruling of ten-inch diffraction gratings. J Opt Soc Am 1959;49(3):205–8.
[14] Harrison GR, Sturgis N, Baker SC, Stroke GW. Ruling of large diffraction gratings with interferometric control. J Opt Soc Am 1957;47(1):15–22.
[15] Hong C, Ibaraki S. Non-contact r-test with laser displacement sensors for error calibration of five-axis machine tools. Precis Eng 2013;37(1):159–71.
[16] Luo X, Cheng K, Webb D, Wardle F. Design of ultraprecision machine tools with applications to manufacture of miniature and micro components. J Mater Process Technol 2005;167(2–3):515–28.
[17] Nawata S, Takashima K. Application of interferometry to the measurement of the pitch of threads on a lead screw. Appl Opt 1966;5(4):609–14.
[18] Han L, Zhang J, Yang F, An Q. Estimation of the gssm calibration error. Appl Opt 2016;55(31):8884–92.
[19] Bao Y, Yi X, Li Z, Chen Q, Li J, Fan X, et al. A digitally generated ultrafine optical frequency comb for spectral measurements with 0.01-pm resolution and 0.7-μs response time. Light Sci Appl 2015;4(6):e300.

[20] Zheng Y, Bian J, Wang XL, Liu JX, Feng P, Ge HX, et al. Revisiting Newton's rings with a plasmonic optical flat for high-accuracy surface inspection. Light Sci Appl 2016;5(10):e16156.
[21] Baets PD, Degrieck J, Velde FVD, Peteghem APV, et al. Experimental verification of the mechanisms causing stick?slip motion originating from relative deceleration. Wear 2000;243(1-2):48–59.
[22] Menezes PL, Kishore Kailas SV. Influence of inclination angle of plate on friction, stick-slip and transfer layer—a study of magnesium pin sliding against steel plate. Wear 2009;267(1–4):476–84.
[23] Wei PJ, Tsai PW, Lin JF. Analysis based on microcontact mechanism for the roughness dependent stick-slip motion. Wear 2009;266(1–2):310–5.